

KANAZAWA-15-06

May, 2015

Constrained inflaton due to a complex scalar

Romy H. S. Budhi ^{1,2,*}, Shoichi Kashiwase ^{2,†},
and
Daijiro Suematsu ^{2,‡}

¹*Physics Department, Gadjah Mada University, Yogyakarta 55281, Indonesia*

²*Institute for Theoretical Physics, Kanazawa University, Kanazawa 920-1192, Japan*

Abstract

We reexamine inflation due to a constrained inflaton in the model of a complex scalar. Inflaton evolves along a spiral-like valley of special scalar potential in the scalar field space just like single field inflation. Sub-Planckian inflaton can induce sufficient e -foldings because of a long slow-roll path. In a special limit, the scalar spectral index and the tensor-to-scalar ratio has equivalent expressions to the inflation with monomial potential φ^n . The favorable values for them could be obtained by varying parameters in the potential. This model could be embedded in a certain radiative neutrino mass model.

*e-mail: romyhanang@hep.s.kanazawa-u.ac.jp

†e-mail: shoichi@hep.s.kanazawa-u.ac.jp

‡e-mail: suematsu@hep.s.kanazawa-u.ac.jp

1 Introduction

Inflationary expansion of the Universe is now believed to have existed before the radiation dominated era in the early Universe [1, 2]. Although a lot of inflation models have been proposed by now [3], we do not know which model can describe this phenomenon correctly. The relation between inflation and particle physics is also unclear. However, recent results of the CMB observations seem to have ruled out many of them already [2]. This has been done by comparing both values of the scalar spectral index and the tensor-to-scalar ratio obtained from the CMB observations and predicted values for them by each model.

If we take a large inflaton scenario in the slow-roll inflation framework, trans-Planckian values are required for realization of sufficient e -foldings. In that case, we cannot answer the question why higher non-renormalizable terms do not contribute to the inflaton potential. If we include such terms in inflaton potential, slow-roll conditions cannot be satisfied. However, such kind of difficulty can be reconciled by compactifying the inflaton trajectory into a winding trajectory in the higher dimensional fields space. In that case, sufficient e -foldings along the trajectory can be obtained even if each field is kept in sub-Planckian regions. That possibility was studied in [4] by introducing an idea about a *spiralized inflation* in two-dimensional field space as a possible solution of the multifield slow-roll inflation. Its realizations have been proposed in the several frameworks, such as in string models [5], SUSY models [6], axions-based models [7, 10, 11, 8, 9] and a complex scalar model which has similar features with axions-based models [12, 13]. The higher order corrections to the potential realizing the spiralized inflation are found to affect significantly the predicted tensor-to-scalar ratio without changing the spectral index substantially [14].

In this paper we study an inflation model based on large but sub-Planckian inflaton. The model considered here has been proposed in [15]. It could have an intimate connection to neutrino mass generation. Although the required number for e -foldings is found to be realized in this model, the predicted tensor-to-scalar ratio by the model is too large compared with a central value of the up-dated observational results [2, 16]. Our main purpose is to study whether the favorable values for them can be obtained in this model. We also discuss a possible connection to a certain particle physics model.

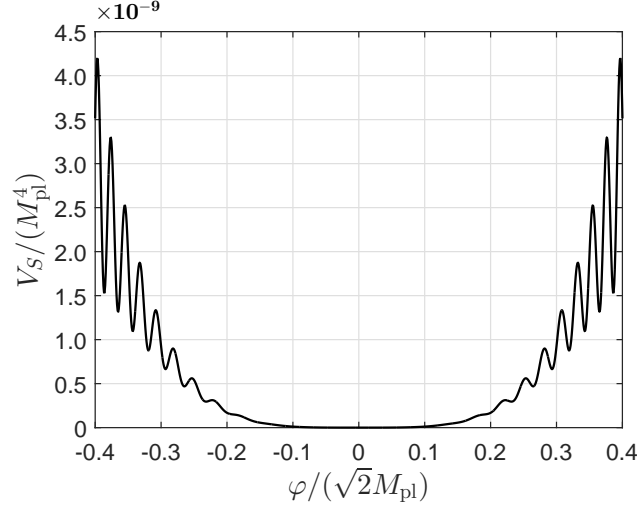


Fig. 1: Potential V_S at a fixed θ for $n = 2, m = 1$ case. Other parameters are fixed at $c_1 = 1.1791 \times 10^{-7}$, $c_2 = 1.4$ and $\Lambda = 0.05 M_{\text{pl}}$.

2 A sub-Planckian inflaton model

The model studied here is defined by a complex scalar S which has Z_2 odd parity. Its Z_2 invariant potential is assumed to be given such as [15]

$$V_S = c_1 \frac{(S^\dagger S)^n}{M_{\text{pl}}^{2n-4}} \left[1 + c_2 \left\{ \left(\frac{S}{M_{\text{pl}}} \right)^{2m} \exp \left(i \frac{S^\dagger S}{\Lambda^2} \right) + \left(\frac{S^\dagger}{M_{\text{pl}}} \right)^{2m} \exp \left(-i \frac{S^\dagger S}{\Lambda^2} \right) \right\} \right].$$

If we use the polar coordinate $S = \frac{\varphi}{\sqrt{2}} e^{i\theta}$, this potential can be written as

$$V_S = c_1 \frac{\varphi^{2n}}{2^n M_{\text{pl}}^{2n-4}} \left[1 + 2c_2 \left(\frac{\varphi}{\sqrt{2} M_{\text{pl}}} \right)^{2m} \cos \left(\frac{\varphi^2}{2\Lambda^2} + 2m\theta \right) \right], \quad (1)$$

where c_2 is assumed to satisfy $c_2 < 0.5 \left(\frac{\varphi}{\sqrt{2} M_{\text{pl}}} \right)^{-2m}$. As shown in Fig. 1, V_S has local minima with a potential barrier $V_b \simeq \frac{c_1 c_2 \varphi^{2(n+m)}}{2^{n+m-2} M_{\text{pl}}^{2(n+m-2)}}$ in the radial direction. These minima form a spiral-like valley whose slope in the angular direction could be extremely small. As a result, if we use the field evolution along this valley, slow-roll inflation is expected to be caused even for sub-Planckian values of φ [15, 13].

The evolution of the scalar field $S = \frac{1}{\sqrt{2}}(\varphi_1 + i\varphi_2)$ in this potential is dictated by the following equation of motion:

$$\ddot{\varphi}_i + 3H\dot{\varphi}_i = -\frac{\partial V_S}{\partial \varphi_i} \quad (i = 1, 2), \quad (2)$$

where the Hubble parameter H of the system is now written as $H^2 = \frac{1}{3M_{\text{pl}}^2} (\sum_i \frac{1}{2} \dot{\varphi}_i^2 + V_S)$ and $\frac{\partial V_S}{\partial \varphi_i}$ denotes partial derivative of the potential V_S in the direction of field component

φ_i . Taking $m = 1$, the terms $\frac{\partial V_S}{\partial \varphi_i}$ could be simply written for any number of n as follows,

$$\begin{aligned} \frac{\partial V_S}{\partial \varphi_1} = \frac{c_1 (S^\dagger S)^n}{M_{\text{pl}}^{2n-4}} & \left[\frac{n\varphi_1}{(S^\dagger S)} + \frac{c_2 \varphi_1}{M_{\text{pl}}^2} \left\{ \frac{n(\varphi_1^2 - \varphi_2^2)}{(S^\dagger S)} + 2 - \frac{2\varphi_1 \varphi_2}{\Lambda^2} \right\} \cos \left(\frac{S^\dagger S}{\Lambda^2} \right) \right. \\ & \left. - \frac{c_2 \varphi_1}{M_{\text{pl}}^2} \left\{ \frac{2n\varphi_1 \varphi_2}{(S^\dagger S)} + 2 \frac{\varphi_2}{\varphi_1} + \frac{(\varphi_1^2 - \varphi_2^2)}{\Lambda^2} \right\} \sin \left(\frac{S^\dagger S}{\Lambda^2} \right) \right], \quad (3) \end{aligned}$$

$$\begin{aligned} \frac{\partial V_S}{\partial \varphi_2} = \frac{c_1 (S^\dagger S)^n}{M_{\text{pl}}^{2n-4}} & \left[\frac{n\varphi_2}{(S^\dagger S)} + \frac{c_2 \varphi_2}{M_{\text{pl}}^2} \left\{ \frac{n(\varphi_1^2 - \varphi_2^2)}{(S^\dagger S)} - 2 - \frac{2\varphi_1 \varphi_2}{\Lambda^2} \right\} \cos \left(\frac{S^\dagger S}{\Lambda^2} \right) \right. \\ & \left. - \frac{c_2 \varphi_2}{M_{\text{pl}}^2} \left\{ \frac{2n\varphi_1 \varphi_2}{(S^\dagger S)} + 2 \frac{\varphi_1}{\varphi_2} + \frac{(\varphi_1^2 - \varphi_2^2)}{\Lambda^2} \right\} \sin \left(\frac{S^\dagger S}{\Lambda^2} \right) \right]. \quad (4) \end{aligned}$$

We may solve eq. (2) numerically to see the evolution of φ_i . The initial value of each component φ_i cannot be selected arbitrarily since the slow-roll behavior could be ruined depending on it. If the initial position of the inflaton is located at a point higher than its next potential barrier, the inflaton could cross over it without realizing the slow-roll motion along the angular direction. The most simple setting for the initial value to realize the slow-roll is to take it at a potential minimum. An example of the evolution of the scalar field components is illustrated in Fig. 2.

Now we describe features of the inflation induced by this field evolution in detail. The radial component φ is assumed to take a large initial value on a local minimum in the radial direction. Even if φ is not just on this minimum initially, it converges to a minimum point within a certain period of time as long as it starts to roll from the neighborhood of a minimum point of the valley initially. In that case, as shown in [15], the model could cause sufficient e -foldings through the inflaton evolution along this spiral-like valley even for sub-Planckian values of φ . An inflaton field χ could be identified with

$$\chi \equiv a_e + \frac{\varphi_e^3}{6m\Lambda^2} - a = \frac{\varphi^3}{6m\Lambda^2}, \quad (5)$$

where the subscript e of the fields stands for the field value at the end of single field inflation. The field a is defined by using φ as

$$da = \left[\varphi^2 + \left(\frac{d\varphi}{d\theta} \right)^2 \right]^{1/2} d\theta = \left[1 + 4m^2 \left(\frac{\Lambda}{\varphi} \right)^4 \right]^{1/2} \varphi d\theta. \quad (6)$$

The number of e -foldings caused by χ during its slow-roll is given as

$$N = -\frac{1}{M_{\text{pl}}^2} \int_{\chi}^{\chi_e} d\chi \frac{V_S}{V'_S} \equiv N(\chi) - N(\chi_e), \quad (7)$$

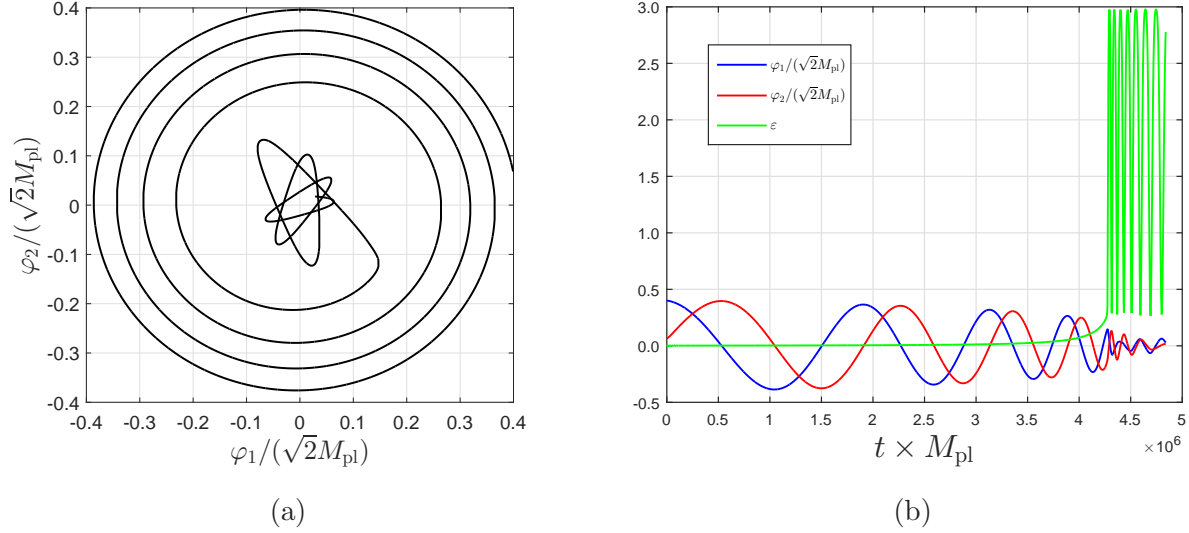


Fig. 2: Inflation evolution for $n = 2, m = 1$ case. Parameters in the potential are fixed at the same values as the ones used in Fig. 1. Inflaton is assumed to be at a potential minimum initially. In this case, it is numerically proven that the end of single field inflation signed as turning point in the panel (a) is mostly realized much before $\epsilon \simeq 1$, such that it is illustrated in the panel (b).

where $V'_S = \frac{dV_S}{d\chi}$ and $N(\chi)$ is represented by using the hypergeometric function F as

$$N(\chi) = \frac{1}{6m^2n} \left(\frac{M_{\text{pl}}}{\Lambda} \right)^4 \left(\frac{\varphi}{\sqrt{2}M_{\text{pl}}} \right)^6 \left[1 + \frac{6c_2m}{n(3+m)} \left(\frac{\varphi}{\sqrt{2}M_{\text{pl}}} \right)^{2m} \right. \\ \left. \times F \left(1, \frac{3}{m} + 1, \frac{3}{m} + 2, 2c_2 \left(1 + \frac{m}{n} \right) \left(\frac{\varphi}{\sqrt{2}M_{\text{pl}}} \right)^{2m} \right) \right]. \quad (8)$$

Slow-roll parameters $\epsilon \equiv \frac{M_{\text{pl}}^2}{2} \left(\frac{V'_S}{V_S} \right)^2$ and $\eta \equiv M_{\text{pl}}^2 \left(\frac{V''_S}{V_S} \right)$ for single field inflation can be represented by using the model parameters as

$$\epsilon = m^2 \left(\frac{\sqrt{2}M_{\text{pl}}}{\varphi} \right)^6 \left(\frac{\Lambda}{M_{\text{pl}}} \right)^4 \left[\frac{n - 2c_2(m+n) \left(\frac{\varphi}{\sqrt{2}M_{\text{pl}}} \right)^{2m}}{1 - 2c_2 \left(\frac{\varphi}{\sqrt{2}M_{\text{pl}}} \right)^{2m}} \right]^2, \\ \eta = m^2 \left(\frac{\sqrt{2}M_{\text{pl}}}{\varphi} \right)^6 \left(\frac{\Lambda}{M_{\text{pl}}} \right)^4 \frac{n(2n-3) - 2c_2(m+n)(2m+2n-3) \left(\frac{\varphi}{\sqrt{2}M_{\text{pl}}} \right)^{2m}}{1 - 2c_2 \left(\frac{\varphi}{\sqrt{2}M_{\text{pl}}} \right)^{2m}}. \quad (9)$$

If the c_2 term is neglected in these formulas, we can find very simple formulas for these slow-roll parameters at the time characterized by the inflaton value χ_* . They can be represented by using the e -foldings N_* , which is defined for $N(\chi_*)$ in eq. (7), as

$$\epsilon \simeq \frac{n}{6(N_* + N(\chi_e))}, \quad \eta \simeq \frac{2n-3}{6(N_* + N(\chi_e))}. \quad (10)$$

Thus, the scalar index n_s and the tensor-to-scalar ratio r can be derived as [15]

$$n_s = 1 - 6\varepsilon + 2\eta \simeq 1 - \frac{n+3}{3(N_* + N(\chi_e))}, \quad r = 16\varepsilon \simeq \frac{8n}{3(N_* + N(\chi_e))}. \quad (11)$$

In order to see the features of this model, it may be useful to compare the model with single field inflation with monomial potential $\varphi^{\bar{n}}$. Since the e -foldings in this model is written as $N \simeq \frac{1}{2\bar{n}} \frac{\varphi^2}{M_{\text{pl}}^2}$, the sufficient e -foldings require a trans-Planckian value for the inflaton φ . We note that the contribution of φ_e is negligible in this case. If we use this number of e -foldings $N_* \simeq N(\varphi_*)$, the slow roll parameters are expressed as

$$\varepsilon = \frac{\bar{n}}{4N_*}, \quad \eta = \frac{\bar{n}-1}{2N_*}, \quad (12)$$

and then n_s and r can be written as

$$n_s = 1 - \frac{\bar{n}+2}{2N_*}, \quad r = \frac{4\bar{n}}{N_*}. \quad (13)$$

It is easily found that n_s and r in both models have the same expression for $\bar{n} = \frac{2}{3}n$ in the limit $c_2 = 0$. However, we should remind that the present model works well only for the non-negligible c_2 since this term causes the potential barrier V_b in the radial direction. V_b makes the inflaton a evolve along the spiral-like trajectory formed by the potential minima like a single field inflation. This brings about a different feature for the model from the $\varphi^{\bar{n}}$ inflation scenario.

In this model, the single field inflation is expected to end at the time when $\frac{1}{2}\dot{\chi}^2 \simeq V_b$ is realized. If we apply the slow-roll approximation $3H\dot{\chi} = -V'_S$ to the slow-roll parameter ε , the inflation is found to end at $\varepsilon = \frac{3V_b(V_b+V_S)}{V_S^2}$. Since $V_S > V_b$ is satisfied, the end of inflation could happen much before the time when $\varepsilon \simeq 1$ is realized. In such a case, $N(\chi) \gg N(\chi_e)$ is not satisfied and then $N(\chi_e)$ has a substantial contribution to determine the number of e -foldings N_* in eq. (7). Thus, the smaller N_* could be enough to realize the same values for n_s and r in comparison with the $\varphi^{\bar{n}}$ inflation.*. We should also note that the values of n_s and r in this model could deviate largely from ones predicted in the $\varphi^{\bar{n}}$ inflation model due to the non-negligible contribution from the c_2 term. Illustration given in Fig. 2b justifies this argument numerically when whole contributions, including non-negligible c_2 term, are taken in to account. As it is expected, the end of inflation at

* Although this becomes clear especially in the small c_2 case, φ_e could be well approximated as the φ value at $\varepsilon = 1$ in other cases.

which inflaton starts to oscillate around global minimum of the potential takes place much before $\varepsilon \simeq 1$. After this time, the inflaton falls in the reheating process and produces lighter particles.

3 Spectral index

We estimate the scalar spectral index n_s and the tensor-to-scalar ratio r by taking account of the $c_2 \neq 0$ effect. Before it, we constrain parameters in the potential by using the normalization for the scalar perturbation found in the CMB. The normalization for the scalar perturbation found in the CMB observations gives the constraint on the inflaton potential V_S at the time when the scale characterized by a certain wave number k_* exits the horizon. The observation of CMB requires the spectrum of scalar perturbation $\mathcal{P}_{\mathcal{R}}(k) = A_s \left(\frac{k}{k_*}\right)^{n_s-1}$ to take $A_s \simeq 2.43 \times 10^{-9}$ at $k_* = 0.002 \text{ Mpc}^{-1}$ [1], V_S should satisfy

$$\frac{V_S}{\varepsilon} = (0.0275 M_{\text{pl}})^4, \quad (14)$$

where we use $A_s = \frac{V_S}{24\pi^2 M_{\text{pl}}^4 \varepsilon}$. If the c_2 term does not dominate the potential, we can represent the condition from this normalization constraint as $c_1 \simeq 9.5 \times 10^{-8} \frac{n}{N_*} \left(\frac{\sqrt{2} M_{\text{pl}}}{\varphi_*}\right)^{2n}$ where φ_* is a value of φ at the time when the e -foldings is N_* .

On the other hand, the e -foldings N_* expected after the scale k_* exits the horizon is dependent on the reheating phenomena and others in such a way as [3]

$$N_* \simeq 61.4 - \ln \frac{k_*}{a_0 H_0} - \ln \frac{10^{16} \text{ GeV}}{V_{k_*}^{1/4}} + \ln \frac{V_{k_*}^{1/4}}{V_{\text{end}}^{1/4}} - \frac{1}{3} \ln \frac{V_{\text{end}}^{1/4}}{\rho_{\text{reh}}^{1/4}}. \quad (15)$$

This suggests that N_* should be considered to have a value in the range 50 - 60. Taking these constraints into account, we estimate both n_s and r for the case where N_* is in this range.

Numerical examples are shown in Table 1 for the cases $n = 1, 2, 3$ with a fixed Λ .[†] For given values of c_2 , the values of c_1 and φ_* are fixed so that the normalization condition given in eq. (14) is satisfied and also N_* takes its value in the imposed range 50 - 60. Both n_s and r are estimated for them.[‡] In Fig. 3, we plot the predicted points in the (n_s, r)

[†] We note that the first term of V_S becomes $c_1 M_{\text{pl}}^2 S^\dagger S$ and $c_1 (S^\dagger S)^2$ for $n = 1$ and 2, respectively.

[‡] If we apply the value of A_s at $k_* = 0.05 \text{ Mpc}^{-1}$ [2] to the present analysis using the same values of $c_{1,2}$ and Λ , φ_* and N_* are changed. This effect on r is found to be $r_{0.05} \simeq 1.07 r_{0.002}$ for the fixed values of c_1 and c_2 which give $n_s \simeq 0.971$ and $r_{0.002} \simeq 0.1$ at $k_* = 0.002 \text{ Mpc}^{-1}$.

n	c_1	c_2	$\frac{\Lambda}{M_{\text{pl}}}$	$\frac{\varphi_1^*}{\sqrt{2}M_{\text{pl}}}$	H_* ($\times 10^{13}\text{GeV}$)	N_*	n_s	r	n'_s
3	1.00×10^{-6}	1.5	0.05	0.417	6.528	60.0	0.967	0.070	-0.00047
	9.84×10^{-7}	1.7	0.05	0.411	5.914	60.0	0.964	0.056	-0.00043
	8.62×10^{-7}	1.9	0.05	0.406	5.399	60.0	0.959	0.040	-0.00032
2	1.32×10^{-7}	1.1	0.05	0.394	7.019	60.0	0.973	0.058	-0.00043
	1.76×10^{-7}	1.1	0.05	0.384	6.725	50.0	0.968	0.072	-0.00061
	1.22×10^{-7}	1.6	0.05	0.383	5.931	60.0	0.969	0.039	-0.00040
	1.71×10^{-7}	1.6	0.05	0.374	5.767	50.0	0.964	0.052	-0.00059
	1.03×10^{-7}	1.9	0.05	0.374	5.318	60.0	0.963	0.026	-0.00035
1	1.36×10^{-8}	0.5	0.05	0.349	5.079	50.0	0.975	0.041	-0.00046
	7.45×10^{-9}	1.6	0.05	0.333	4.146	60.0	0.970	0.015	-0.00036
	1.02×10^{-9}	1.6	0.05	0.326	4.102	50.0	0.966	0.019	-0.00052
	6.15×10^{-9}	1.8	0.05	0.327	3.976	60.0	0.966	0.011	-0.00035
	8.77×10^{-9}	1.8	0.05	0.320	3.944	50.0	0.962	0.016	-0.00052

Table 1 Examples of the predicted values for the spectral index n_s and the tensor-to-scalar ratio r in this scenario with $m = 1$.

plane by red and green circles, which correspond to $N_* = 50$ and 60 respectively for every 0.1 of c_2 starting from $c_2 = 0.1$ on the right-hand side while Λ is fixed as $\Lambda = 0.05M_{\text{pl}}$. We show the boundary values of c_2 by the red and black stars, for which either red or green circles are inside of the region of 2σ CL and 1σ CL of the latest Planck TT+lowP+BKP+lensing+ext combined data for the $n = 3$ and $n = 1, 2$ panels, respectively. They show that the present model with c_2 included in this interval are favored by the latest Planck data combined with others. The best fit result is obtained for the $n = 1$ case.

As discussed above, the present model shows the similar behavior to the monomial inflation models at least for the spectral index and the tensor-to-scalar ratio in the limiting case with the negligible c_2 . However, if c_2 is not negligible, this feature could be changed and these values largely deviate from the monomial inflation models. Since the predicted region in the (n_s, r) plane could be distinctive from other inflation models, the model might be tested through future CMB observations. One of the promising CMB observations would be LiteBIRD which is expected to detect the signal of the gravitational wave with

$r > 0.01$ at more than 10σ [17]. Thus the whole of the predicted region could be verified in near future.

Recent CMB results suggest that the running of the spectral index is consistent with zero at 1σ level. Thus, this can be an another useful test of the model. The running of the spectral index is known to be expressed by using the slow-roll parameters as

$$n'_s \equiv \frac{dn_s}{d \ln k} \simeq -24\varepsilon^2 + 16\varepsilon\eta - 2\xi^2, \quad (16)$$

where ξ is defined as $\xi^2 \equiv M_{\text{pl}}^4 \frac{V'_S V''_S}{V_S^2}$. In the present model, it is written by using the model parameters as

$$\begin{aligned} \xi^2 = & 2m^4 \left(\frac{\sqrt{2}M_{\text{pl}}}{\varphi} \right)^{12} \left(\frac{\Lambda}{M_{\text{pl}}} \right)^8 \left[\frac{n - 2c_2(n+m) \left(\frac{\varphi}{\sqrt{2}M_{\text{pl}}} \right)^{2m}}{1 - 2c_2 \left(\frac{\varphi}{\sqrt{2}M_{\text{pl}}} \right)^{2m}} \right. \\ & \times \left. \frac{n(n-3)(2n-3) - 2c_2(n+m)(n+m-3)(2n+2m-3) \left(\frac{\varphi}{\sqrt{2}M_{\text{pl}}} \right)^{2m}}{1 - 2c_2 \left(\frac{\varphi}{\sqrt{2}M_{\text{pl}}} \right)^{2m}} \right]. \quad (17) \end{aligned}$$

If we use the parameters given in Table 1, the running of the spectral index can be estimated in each case by using these formulas. The results are shown in the last column of Table 1. Although they are consistent with the latest Planck data, they take very small negative values. We might be able to use it for the verification of the model in future.

4 Relation with particle physics

Finally, we discuss the relation of the model with particle physics. Although we cannot clarify the origin of potential (1) at the present stage, we expect it might be produced through some non-perturbative effects of Planck scale physics. The complex scalar S can play an important role in particle physics if we embed it in an extended standard model. As such an interesting example, we consider the radiative neutrino mass model proposed by Ma [18]. This model is given by the following Lagrangian for the neutrino sector:

$$\begin{aligned} -\mathcal{L} = & \sum_{\alpha,k=1}^3 \left(h_{\alpha k} \bar{N}_k \eta^\dagger \ell_\alpha + h_{\alpha k}^* \bar{\ell}_\alpha \eta N_k + \frac{M_k}{2} \bar{N}_k N_k^c + \frac{M_k}{2} \bar{N}_k^c N_k \right) \\ & + m_\phi^2 \phi^\dagger \phi + m_\eta^2 \eta^\dagger \eta + \lambda_1 (\phi^\dagger \phi)^2 + \lambda_2 (\eta^\dagger \eta)^2 + \lambda_3 (\phi^\dagger \phi) (\eta^\dagger \eta) + \lambda_4 (\eta^\dagger \phi) (\phi^\dagger \eta) \\ & + \frac{\lambda_5}{2} [(\eta^\dagger \phi)^2 + (\phi^\dagger \eta)^2], \quad (18) \end{aligned}$$

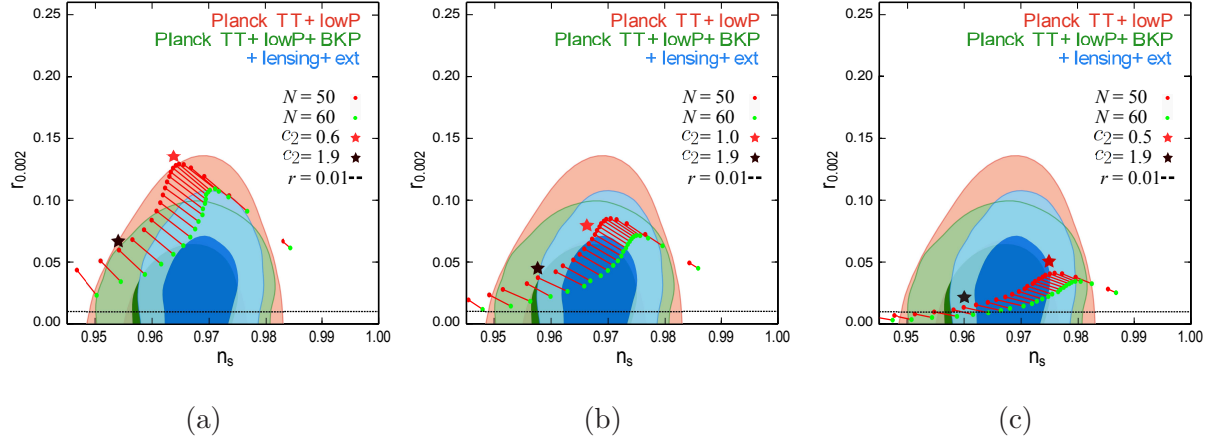


Fig. 3: Predicted regions in the (n_s, r) plane are presented in panel (a) for $n = 3$, in panel (b) for $n = 2$, and in panel (c) for $n = 1$. Λ is fixed as $\Lambda = 0.05 M_{\text{pl}}$ in all cases. The values of c_1 and φ_* are given in Table 1 for representative values of c_2 . Contours given in the right panel of Fig. 21 in Planck 2015 results.XIII.[2] are used here. Horizontal black lines $r = 0.01$ represent a possible limit detected by LiteBIRD in near future.

where ℓ_α and ϕ are the doublet leptons and the ordinary doublet Higgs scalar in the standard model. Two types new fields are introduced in this model, that is, an inert double scalar η and singlet fermions N_k . All their masses are assumed to be of $O(1)$ TeV. New fields η and N_k are assigned odd parity of imposed Z_2 symmetry, although all the standard model contents have its even parity. Since η is assumed to have no vacuum expectation value, this Z_2 symmetry is exact and then neutrino masses cannot be generated at tree level. Neutrinos get masses through a one-loop diagram which has η and N_k in the internal lines as shown in the left-hand diagram of Fig.4. Moreover, the lightest neutral Z_2 odd field is stable to be a good dark matter (DM) candidate. Thus, DM is an inevitable ingredient for the neutrino mass generation in this model. The model has been clarified quantitatively to have interesting features through a lot of studies [19, 20].

We can relate the present model to the Ma model by identifying the Z_2 symmetry in the present model with that in the Ma model. We assign its odd parity to the complex scalar S . If we take account of these symmetry, new terms which are subdominant during the inflation period are introduced as invariant ones,

$$\begin{aligned}
-\mathcal{L}_S &= \tilde{m}_S^2 S^\dagger S + \frac{1}{2} m_S^2 S^2 + \frac{1}{2} m_S^2 S^{\dagger 2} + \kappa_1 (S^\dagger S)^2 + \kappa_2 (S^\dagger S)(\phi^\dagger \phi) + \kappa_3 (S^\dagger S)(\eta^\dagger \eta) \\
&- \mu S \eta^\dagger \phi - \mu S^\dagger \phi^\dagger \eta.
\end{aligned} \tag{19}$$

Here we note that the λ_5 term in eq. (18) is also allowed under the imposed symmetry.

However, since its β -function is proportional to itself if an interaction $\mu S \eta^\dagger \phi$ in the last line of eq. (19) is neglected, $\lambda_5 = 0$ is stable for radiative corrections. On the other hand, if it is included in the Lagrangian, the λ_5 term can be induced through this interaction as the effective one at low energy regions after integrating out the heavy S field.

This can be easily seen through the neutrino mass generation. In the present extended model, the neutrino masses can be generated through the right-hand diagram of Fig. 4. The neutrino masses obtained through this diagram can be described by the formula

$$(\mathcal{M}_\nu)_{\alpha\beta} = \sum_{k=1}^3 \sum_{a=1,2} \frac{h_{\alpha k} h_{\beta k} M_k \mu_a^2 \langle \phi \rangle^2}{8\pi^2} I(M_\eta, M_k, m_{\varphi_a}), \quad (20)$$

where $M_\eta^2 = m_\eta^2 + (\lambda_3 + \lambda_4) \langle \phi \rangle^2$ and m_{φ_a} represents the mass of the real and imaginary component of S which can be expressed as $m_{\varphi_1}^2 = \tilde{m}_S^2 + m_S^2$ and $m_{\varphi_2}^2 = \tilde{m}_S^2 - m_S^2$. μ_a stands for $\mu_1 = \frac{\mu}{\sqrt{2}}$ and $\mu_2 = \frac{i\mu}{\sqrt{2}}$, respectively. The function $I(m_a, m_b, m_c)$ is defined as

$$\begin{aligned} I(m_a, m_b, m_c) &= \frac{(m_a^4 - m_b^2 m_c^2) \ln m_a^2}{(m_b^2 - m_a^2)^2 (m_c^2 - m_a^2)^2} + \frac{m_b^2 \ln m_b^2}{(m_c^2 - m_b^2)(m_a^2 - m_b^2)^2} \\ &+ \frac{m_c^2 \ln m_c^2}{(m_b^2 - m_c^2)(m_a^2 - m_c^2)^2} - \frac{1}{(m_b^2 - m_a^2)(m_c^2 - m_a^2)}. \end{aligned} \quad (21)$$

If $m_{\varphi_a}^2 \gg M_k^2$, M_η^2 is satisfied and it corresponds to the present case, this formula is found to be reduced to

$$\mathcal{M}_{\alpha\beta}^\nu \simeq \left(\sum_{a=1,2} \frac{\mu_a^2}{m_{\varphi_a}^2} \right) \sum_{k=1}^3 \frac{h_{\alpha k} h_{\beta k} \langle \phi \rangle^2}{8\pi^2} \frac{M_k}{M_\eta^2 - M_k^2} \left[1 + \frac{M_k^2}{M_\eta^2 - M_k^2} \ln \frac{M_k^2}{M_\eta^2} \right], \quad (22)$$

which is equivalent to the neutrino mass formula obtained through the left-hand diagram of Fig. 4 for the Ma model. This shows that λ_5 can be identified with $\sum_a \frac{\mu_a^2}{m_{\varphi_a}^2}$ as the effective coupling obtained at the low energy regions much smaller than m_{φ_a} . The key coupling for the neutrino mass generation in the Ma model could be closely related to the inflaton interaction term in this extension.

We should also note that the interesting feature for DM in the Ma model is completely kept in this extended model. We suppose that the Z_2 odd lightest field is the neutral real component of the inert doublet η_R . Its stability is guaranteed by the imposed Z_2 symmetry. Since its relic abundance is determined by the coannihilations among the components of η which are controlled by the coupling constants $\lambda_{3,4}$ in eq. (18), the results obtained in [23, 24] can be applied to the present model without affecting the analysis in

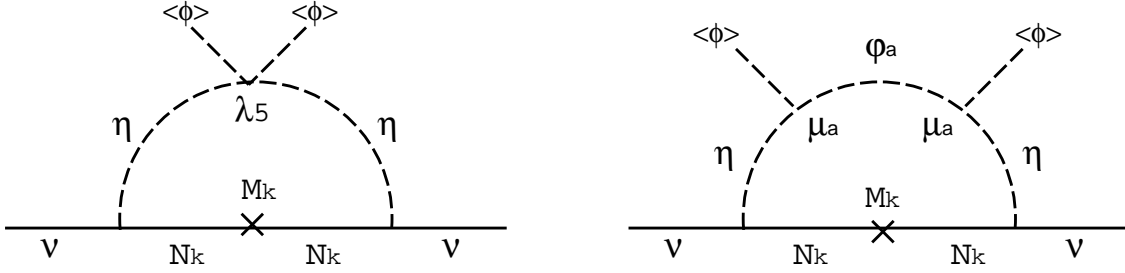


Fig. 4: One-loop diagrams contributing to the neutrino mass generation. The left-hand diagram is the one in the Ma model. Lepton number is violated through the Majorana mass of N_K . The right-hand diagram is the one in the present extended model. φ_a represents the real and imaginary part of the singlet scalar S defined by $S = \frac{1}{\sqrt{2}}(\varphi_1 + i\varphi_2)$. μ_a is a dimensional coupling for φ_a which is expressed as $\mu_1 = \frac{\mu}{\sqrt{2}}$ and $\mu_2 = \frac{i\mu}{\sqrt{2}}$.

this paper. They shows the required relic abundance $\Omega h^2 = 0.12$ could be easily realized if either λ_3 or λ_4 takes a value of $O(1)$ for the η_R with the mass of $O(1)$ TeV. Thus, this extended model could give a simple explanation not only for the inflation but also for the neutrino masses and the DM abundance, simultaneously.

5 Summary

We have considered an inflation scenario based on a complex singlet scalar. Special potential of this scalar constrains the inflaton evolution along a spiral-like trajectory in the space of two degrees of freedom. This makes the model behave like a single field inflation scenario. However, since the slope along this constrained direction is flat enough, inflaton can travel through trans-Planckian path. As a result, the sufficient e -foldings can be realized even for sub-Planckian inflaton values. Serious potential problem in the large field inflaton could be solved in this model. Both the spectral index and the tensor-to-scalar ratio predicted in this model can be consistent with recently up-dated CMB observational results. Since these could take values in distinctive regions from other inflation scenario, the model might be tested through future CMB observations.

The inflaton in this model might be embedded into the extended standard model as an important ingredient. As such an example, we have discussed a possibility that the inflaton is an indispensable element in the radiative neutrino mass model, where a certain quartic scalar coupling plays a crucial role in the neutrino mass generation. Since the inflaton causes this coupling as an effective one at low energy regions, it could have a

close relation with particle physics in this extension. The model might have another interesting feature. Reheating through the inflaton decay might give the origin of baryon number asymmetry through the generation of the lepton number asymmetry in a non-thermal way. Detailed study of this subject will be presented in future publication [22]. If it could be shown through explicit analysis, the problems in the standard model might be solved in a compact way in this extended model.

Acknowledgement

R. H. S. Budhi is supported by the Directorate General of Higher Education (DGHE) of Indonesia (Grant Number 1245/E4.4/K/2012). S. K. is supported by Grant-in-Aid for JSPS fellows (26-5862). D. S. is supported by JSPS Grant-in-Aid for Scientific Research (C) (Grant Number 24540263) and MEXT Grant-in-Aid for Scientific Research on Innovative Areas (Grant Number 26104009).

References

- [1] WMAP Collaboration, D. N. Spergel, *et al.*, *First year Wilkinson Microwave Anisotropy Probe (WMAP) observations: Determination of cosmological parameters*, *Astrophys. J. Suppl.* **148** (2003) 175 [astro-ph/0302209];
- E. Komatsu, *et al.*, *Five-Year Wilkinson Microwave Anisotropy Probe (WMAP) Observations: Cosmological Interpretation*, *Astrophys. J. Suppl.* **180** (2009) 330 [arXiv:0803.0547 [astro-ph]];
- E. Komatsu, *et al.*, *Seven-Year Wilkinson Microwave Anisotropy Probe (WMAP) Observations: Cosmological Interpretation*, *Astrophys. J. Suppl.* **192** (2011) 18 [arXiv:1001.4538[astro-ph.CO]];
- G. Hinshaw, *et al.*, *Nine-Year Wilkinson Microwave Anisotropy Probe (WMAP) Observations: Cosmological Parameter Results*, *Astrophys. J. Suppl.* **208** (2013) 19 [arXiv:1212.5226 [astro-ph.CO]];
- Planck Collaboration, P. A. R. Ade, *et al.*, *Planck 2013 results. XXII. Constraints on inflation*, *Astron. Astrophys.* **571** (2014) A22 [arXiv:1303.5082 [astro-ph.CO]].

- [2] Planck Collaboration, P. A. R. Ade, *et al.*, *Planck 2015 results. XIII. Cosmological parameters*, [arXiv:1502.01589 [astro-ph.CO]];
Planck Collaboration, P. A. R. Ade, *et al.*, *Planck 2015 results. XX. Constraints on inflation*, [arXiv:1502.02114 [astro-ph.CO]].
- [3] For reviews, D. H. Lyth and A. Riotto, *Particle physics models of inflation and the cosmological density perturbation*, *Phys. Rept.* **314** (1999) 1 [hep-ph/9807278];
A. R. Liddle and D. H. Lyth, *Cosmological inflation and Large-Scale Structure*, Cambridge University Press, Cambridge U.K, (2000).
- [4]] I. S. Yang, *The Strong Multifield Slowroll Condition and Spiral Inflation*, *Phys.Rev.* **D85** (2012) 123532 [arXiv:1202.3388 [hep-th]]
- [5] Pontus Ahlqvist, Brian Greene¹, and David Kagan, *Exploring Spiral Inflation in String Theory*, [arXiv:1308.0538 [hep-th]].
- [6] T. Li, Z. Li, D. V. Nanopoulos, *Helical Phase Inflation*, *Phys. Rev.* **D91** (2015) 061303 [arXiv:1409.3267[hep-th]];
T. Li, Z. Li, D. V. Nanopoulos, *Helical Phase Inflation and Monodromy in Supergravity Theory*, [arXiv:1412.5093[hep-th]].
- [7] J. McDonald, *A Minimal Sub-Planckian Axion Inflation Model with Large Tensor-to-Scalar Ratio*, *JCAP* **1501** (2015) 018 [arXiv:1407.7471 [hep-th]]
- [8] C. D. Carone, J. Erlich, A. Sensharma, Z. Wang, *Dante’s Waterfall*, *Phys. Rev.* **D91** (2015) 043512 [arXiv:1410.2593[hep-ph]].
- [9] Marcus Berg, Enrico Pajer, and Stefan Sjors, *Dantes Inferno*, *Phys.Rev.* **D81** (2010) 103535, [arXiv:0912.1341 [hep-th]]
- [10] Jihn E. Kim, , Hans Peter Nilles, and Marco Peloso *Completing Natural Inflation*, *JCAP* **0501** (2005) 005, [arXiv:hep-ph/0409138]
- [11] Rolf Kappl, Sven Krippendorff and Hans Peter Nilles , *Aligned Natural Inflation: Monodromies of two Axions*, *Phys.Lett.* **B737** (2014) 124-128 , [arXiv:1404.7127v3 [hep-th]]

- [12] G. Barenboim, W.-II Park, *Spiral Inflation*, *Phys. Lett.* **B741** (2015) 252 [arXiv:1412.2724[hep-ph]]
 Gabriela Barenboim and Wan-II Park, *Spiral Inflation with Coleman-Weinberg Potential*, *Phys.Rev.* **D91** (2015) 063511, [arXiv:1501.00484 [hep-ph]].
- [13] J. McDonald, *Sub-Planckian Two-Field Inflation Consistent with the Lyth Bound*, *JCAP* **09** (2014) 027 [arXiv:1404.4620 [hep-ph]].
- [14] J. McDonald, *Signatures of Planck Corrections in a Spiralling Axion Inflation Model*, *JCAP* **1505** (2015) 014 [arXiv:1412.6943[hep-ph]].
- [15] R. H. S. Budhi, S. Kashiwase and D. Suematsu, *Inflation in a modified radiative seesaw model*, *Phys. Rev.* **D90** (2014) 113013 [arXiv:1409.6889 [hep-ph]].
- [16] BICEP2/Keck and Planck Collaborations, P. A. R. Ade, *et al.*, *Joint Analysis of BICEP2/KeckArray and Planck Data*, *Phys. Rev. Lett.* **114** (2015) 101301 [arXiv:1502.00612 [astro-ph.CO]].
- [17] M. Hazumi, *Future CMB polarization measurements and Japanese contributions*, *Prog. Theor. Phys. Suppl.* **190** (2011) 75.
- [18] E. Ma, *Verifiable radiative seesaw mechanism of neutrino mass and dark matter*, *Phys. Rev.* **D73** (2006) 077301 [hep-ph/0601225].
- [19] J. Kubo, E. Ma and D. Suematsu, *Cold Dark Matter, Radiative Neutrino Mass, $\mu \rightarrow e\gamma$, and Neutrinoless Double Beta Decay*, *Phys. Lett.* **B642** (2006) 18 [hep-ph/0604114];
 J. Kubo and D. Suematsu, *Neutrino masses and CDM in a non-supersymmetric model*, *Phys. Lett.* **B643** (2006) 336 [hep-ph/0610006]; D. Aristizabal Sierra, J. Kubo, D. Suematsu, D. Restrepo and O. Zapata, *Radiative seesaw: Warm dark matter, collider and lepton flavour violating signals*, *Phys. Rev.* **D79** (2009) 013011 [arXiv:0808.3340 [hep-ph]];
 D. Suematsu, T. Toma and T. Yoshida, *Reconciliation of CDM abundance and $\mu \rightarrow e\gamma$ in a radiative seesaw model*, *Phys. Rev.* **D79** (2009) 093004 [arXiv:0903.0287 [hep-ph]];
 D. Suematsu, T. Toma and T. Yoshida, *Enhancement of the annihilation of dark*

matter in a radiative seesaw model, *Phys. Rev.* **D82** (2010) 013012 [arXiv:1002.3225 [hep-ph]].

- [20] D. Suematsu, *Leptogenesis and dark matter unified in a non-SUSY model for neutrino masses*, *Eur. Phys. J.* **C56** (2008) 379 [arXiv:0706.2401 [hep-ph]];
D. Suematsu, *Thermal Leptogenesis in a TeV Scale Model for Neutrino Masses*, *Eur. Phys. J.* **C72** (2012) 1951 [arXiv:1103.0857 [hep-ph]].
- [21] D. Suematsu, *Extension of a radiative neutrino mass model based on a cosmological view point*, *Phys. Rev.* **D85** (2012) 073008 [arXiv:1202.0656 [hep-ph]].
- [22] S. Kashiwase and D. Suematsu, in preparation.
- [23] T. Hambye, F.-S. Ling, L. L. Honorez and J. Roche, *Scalar Multiplet Dark Matter*, *JHEP* **07** (2009) 090 [arXiv:0903.4010 [hep-ph]].
- [24] S. Kashiwase and D. Suematsu, *Baryon number asymmetry and dark matter in the neutrino mass model with an inert doublet*, *Phys. Rev.* **D86** (2012) 053001 [arXiv:1207.2594 [hep-ph]];
S. Kashiwase and D. Suematsu, *Leptogenesis and dark matter detection in a TeV scale neutrino mass model with inverted mass hierarchy*, *Eur. Phys. J.* **C73** (2013) 2484 [arXiv:1301.2087 [hep-ph]].